SEP 3 0 1974
NOV 1 3 1974

AEDC-TR-74-65

Cy. 4

APPLICATION OF LINEARIZED TRANSONIC THEORY TO TUNNEL BLOCKAGE INTERFERENCE

C. F. Lo
ARO, Inc.

PROPULSION WIND TUNNEL FACILITY
ARNOLD ENGINEERING DEVELOPMENT CENTER
AIR FORCE SYSTEMS COMMAND
ARNOLD AIR FORCE STATION, TENNESSEE 37389

September 1974

Final Report for Period February 1 — November 30, 1973

Approved for public release; distribution unlimited.

[illegible] AIR FORCE
AEDC [illegible]
F40600-75-C-0001

Prepared for

ARNOLD ENGINEERING DEVELOPMENT CENTER (DYFS)
ARNOLD AIR FORCE STATION, TN 37389

NOTICES

When U. S. Government drawings specifications, or other data are used for any purpose other than a definitely related Government procurement operation, the Government thereby incurs no responsibility nor any obligation whatsoever, and the fact that the Government may have formulated, furnished, or in any way supplied the said drawings, specifications, or other data, is not to be regarded by implication or otherwise, or in any manner licensing the holder or any other person or corporation, or conveying any rights or permission to manufacture, use, or sell any patented invention that may in any way be related thereto.

Qualified users may obtain copies of this report from the Defense Documentation Center.

References to named commercial products in this report are not to be considered in any sense as an endorsement of the product by the United States Air Force or the Government.

APPROVAL STATEMENT

This technical report has been reviewed and is approved.

Carlos Tirres

CARLOS TIRRES
Captain, USAF
Research and Development
Division
Directorate of Technology

Robert O Dietz

ROBERT O. DIETZ
Director of Technology

UNCLASSIFIED

SECURITY CLASSIFICATION OF THIS PAGE *(When Data Entered)*

REPORT DOCUMENTATION PAGE		READ INSTRUCTIONS BEFORE COMPLETING FORM
1. REPORT NUMBER AEDC-TR-74-65	2. GOVT ACCESSION NO.	3 RECIPIENT'S CATALOG NUMBER
4 TITLE *(and Subtitle)* APPLICATION OF LINEARIZED TRANSONIC THEORY TO TUNNEL BLOCKAGE INTERFERENCE		5 TYPE OF REPORT & PERIOD COVERED Final Report, Feb. 1 to Nov. 30, 1973 6 PERFORMING ORG. REPORT NUMBER
7. AUTHOR(s) C. F. Lo, ARO, Inc.		8. CONTRACT OR GRANT NUMBER(s)
9 PERFORMING ORGANIZATION NAME AND ADDRESS Arnold Engineering Development Center (DY) Arnold Air Force Station, TN 37389		10 PROGRAM ELEMENT, PROJECT, TASK AREA & WORK UNIT NUMBERS Program Element 65802F
11. CONTROLLING OFFICE NAME AND ADDRESS Arnold Engineering Development Center (DYFS), Arnold AF Station, TN 37389		12. REPORT DATE September 1974 13. NUMBER OF PAGES 28
14 MONITORING AGENCY NAME & ADDRESS(*if different from Controlling Office*)		15. SECURITY CLASS. *(of this report)* UNCLASSIFIED 15e. DECLASSIFICATION/DOWNGRADING SCHEDULE N/A

16 DISTRIBUTION STATEMENT *(of this Report)*

Approved for public release; distribution unlimited.

17 DISTRIBUTION STATEMENT *(of the abstract entered in Block 20, if different from Report)*

18. SUPPLEMENTARY NOTES

Available in DDC.

19 KEY WORDS *(Continue on reverse side if necessary and identify by block number)*

transonic wind tunnels
blockage
interference
transonic flow
subsonic flow
walls, ventilated

20 ABSTRACT *(Continue on reverse side if necessary and identify by block number)*

The tunnel blockage interference is calculated by the application of linearized transonic theory. The linearized transonic perturbation equation is solved by the Fourier transform technique to obtain blockage interference in a perforated transonic wind tunnel in terms of pressure coefficient. The calculation has been used to determine the applicable Mach number range of subsonic tunnel corrections. An application to a circular-arc airfoil is presented to demonstrate the accuracy of the blockage correction.

DD FORM 1 JAN 73 1473 EDITION OF 1 NOV 65 IS OBSOLETE

UNCLASSIFIED

SECURITY CLASSIFICATION OF THIS PAGE *(When Data Entered)*

PREFACE

The work reported herein was conducted by the Arnold Engineering Development Center (AEDC), Air Force Systems Command (AFSC), under Program Element 65802F. The results presented were obtained by ARO, Inc. (a subsidiary of Sverdrup & Parcel and Associates, Inc.), contract operator of AEDC, AFSC, Arnold Air Force Station, Tennessee. The work was conducted under ARO Project Nos. PF210 and PF422, and the manuscript (ARO Control No. ARO-PWT-TR-74-45) was submitted for publication on May 29, 1974.

CONTENTS

		Page
1.0	INTRODUCTION	5
2.0	LINEARIZED TRANSONIC THEORY	6
3.0	TRANSONIC THEORY OF TUNNEL BLOCKAGE INTERFERENCE	
	3.1 Formulation	8
	3.2 Determination of Transonic Acceleration Parameter	10
4.0	INTERFERENCE PRESSURE ON A CIRCULAR ARC AIRFOIL	
	4.1 Interference Pressure Coefficient	12
	4.2 Validity Range of Mach Number for Subsonic Interference Theory	17
	4.3 Application	21
5.0	CONCLUDING REMARKS	23
	REFERENCES	23

ILLUSTRATIONS

Figure		
1.	Wind Tunnel and Model Geometries	7
2.	Interference Pressure Coefficients on a 6-Percent Circular-Arc Airfoil at h/c = 3.0	13
3.	Tunnel Height to Chord Ratio Effect on the Interference Pressure Coefficient of a 6-Percent Circular-Arc Airfoil at Q = 0.6	15
4.	Porosity Effect on the Average Interference Pressure Coefficient, C_{p_i}, of a 6-Percent Circular-Arc Airfoil at h/c = 3.0	17
5.	Comparison of Transonic and Subsonic Theories on Interference Pressure Coefficient at Various Mach Numbers	18
6.	Application of Interference Pressure Coefficient to Closed Tunnel Configuration on a 6-Percent Circular-Arc Airfoil at h/c = 3.4	21

APPENDIXES

Page

A. EVALUATION OF THE INTERFERENCE VELOCITY EXPRESSION 25

B. INTEGRATION OF EXPRESSIONS M_c AND M_s 26

NOMENCLATURE 27

1.0 INTRODUCTION

The interference on the flow field over a model caused by the presence of wind tunnel walls has been recognized ever since wind tunnels were originated. At subsonic speeds, simple formulae for correction factors are available for closed and open-jet tunnels. Since ventilated walls were introduced into transonic wind tunnels, the calculation of correction factors has become rather complicated. Furthermore, as Mach number increases, mixed flow (supersonic and subsonic) regions appear around a model causing complexity of the computations to increase an order of magnitude, especially when the local supersonic region reaches the tunnel walls or Mach number approaches the sonic speed.

Available theoretical correction formulae for ventilated tunnels are based mainly on linearized subsonic theory with compressibility effects accounted for by the Prandtl-Glauert scaling factor (Refs. 1 and 2). The subsonic interference in the perforated tunnels of rectangular cross section has been calculated numerically in Refs. 3 and 4. The compressibility scaling factor in the linearized subsonic theory is valid only for the subcritical flow (i.e., flow without a mixed subsonic and supersonic flow region). However, the subsonic correction theory may be still valid even though the flow over the model becomes supercritical (i.e., even though it has a supersonic region embedded in the flow). Hence, the Mach number range for which the subsonic tunnel theory is applicable needs to be determined.

The application of transonic theory to wind tunnel data corrections is reviewed in Ref. 5, and particularly the axisymmetric case is considered by the equivalence principle. In recent years, several numerical methods have become available for the free-air case (infinite extended flow) and are reviewed in Ref. 6. Similar numerical schemes have been applied to wind tunnel flow problems on a body of revolution model (Ref. 7) and a two-dimensional airfoil (Ref. 8). Both numerical computations solve the complete tunnel flow field around a test model, but neither of them provides tunnel corrections directly. Hence, the solution for the free-air case is required to obtain the difference between tunnel flow and free-air fields for tunnel corrections. These available numerical methods have been utilized in an attempt to determine the range of validity of subsonic wind tunnel corrections for the two-dimensional case (Ref. 9). The only approximate formulation using the local linearized transonic theory was solved by the integral method for a two-dimensional symmetrical airfoil at sonic speed (Ref. 10).

In the present report, the tunnel blockage interference is calculated directly for a two-dimensional symmetrical model in a perforated transonic tunnel using the linearized transonic theory developed by Oswatitsch (Ref. 11) and Maeder and Wood (Ref. 12). This method of direct computation of the interference does not require the exact representation of the model flow at supercritical Mach numbers. It is assumed that the tunnel Mach number is subsonic and that the embedded supersonic region does not extend to the tunnel walls. The transonic small perturbation equation is used. The blockage interference is obtained in terms of pressure coefficient by the Fourier transform technique. The Mach number range for which subsonic tunnel corrections are valid is defined by comparing the present transonic results with subsonic corrections. The computed pressure correction can be applied directly to the measured pressure coefficients on a model. The results may also provide useful information for tunnel wall design and the selection of model size.

2.0 LINEARIZED TRANSONIC THEORY

The linearized transonic theory was first proposed by Oswatitsch (Ref. 11) and later was extended by Maeder and Wood (Ref. 12). The flow is assumed to be inviscid and irrotational. The transonic small perturbation equation for flow over a two-dimensional thin airfoil in Cartesian coordinates of x, y (Fig. 1a) is

$$(1 - M_\infty^2)\phi_{xx} + \phi_{yy} = (\gamma + 1)M_\infty^2\phi_x\phi_{xx} \tag{1}$$

where the velocity potential, ϕ, is normalized with respect to the free-stream velocity, U_∞. The boundary condition of tangential flow at the airfoil surface is of the form

$$\phi_y = rF_x(x) \tag{2}$$

at $y \to 0$. Further, the perturbation velocities vanish at infinity. The linearization of Eq. (1), devised by Oswatitsch-Mader, produces

$$(1 - M_\infty^2)\phi_{xx} + \phi_{yy} = k^2\phi_x \tag{3}$$

where

$$k^2 = (\gamma + 1)M_\infty^2\phi_{xx}$$

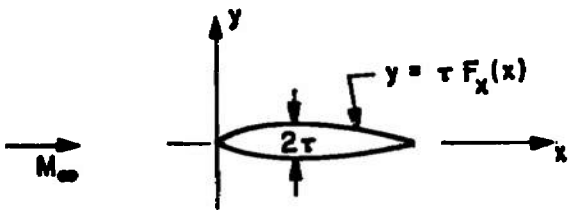

a. Free-air flow.

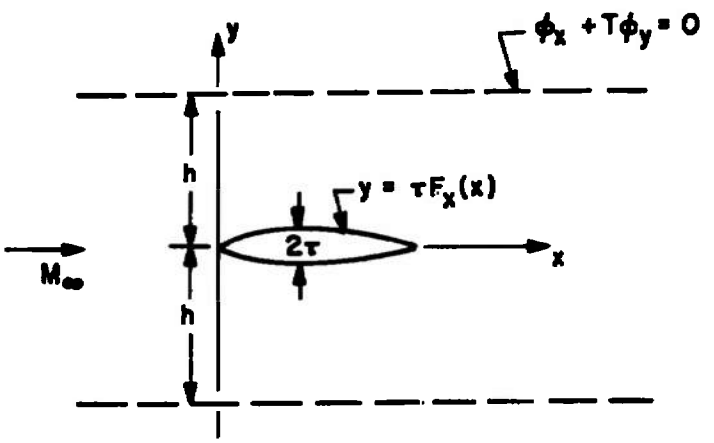

b. Wind tunnel flow

Figure 1. Wind tunnel and model geometries.

The acceleration parameter, ϕ_{xx}, is assumed to be an average constant, $\tilde{\phi}_{xx}$, over a thin airfoil.

For the convenience of tunnel blockage interference calculation, the linearized transonic equation is written in terms of the axial velocity, u, as a dependent function; thus,

$$\beta^2 u_{xx} - u_{yy} = k^2 u_x \tag{4}$$

with boundary conditions

$$u_y = \tau F_{xx} \qquad \text{at} \qquad y \to 0 \tag{5}$$

$$u = u_x = 0 \qquad \text{at} \qquad x, y \to \infty \tag{6}$$

In order to solve the boundary value problem posed in Eqs. (4) through (6), the Fourier transform technique is applied. The boundary value problem in the transformed plane becomes

$$-\beta^2 p^2 \bar{u} + \bar{u}_{yy} = -ik^2 p\bar{u}$$

or

$$\bar{u}_{yy} - \lambda^2 \bar{u} = 0 \tag{7}$$

where

$$\bar{u} = (2\pi)^{-\frac{1}{2}} \int_{-\infty}^{\infty} u(x)\, e^{ipx}\, dx \tag{8}$$

and

$$\lambda^2 = \beta^2 p(p - ik^2) \tag{9}$$

and the boundary condition at $y \to 0$ is given as

$$\bar{u}_y = (2\pi)^{-\frac{1}{2}} \int_{-\infty}^{\infty} \tau F_{xx}\, e^{ipx}\, dx = \tau f(p) \tag{10}$$

The solution of Eqs. (7) and (10) in the transformed plane is

$$\bar{u}(y,p) = -[\tau f(p)/\lambda]\, e^{-\lambda y} \tag{11}$$

The solution in the physical plane can be obtained by the Fourier inversion formula. The detail solution in the physical plane can be found in the report by Maeder and Wood (Ref. 12). However, the transformed solution for free-air flow, Eq. (11), will be used to identify the interference portion of the solution in the following section.

3.0 TRANSONIC THEORY OF TUNNEL BLOCKAGE INTERFERENCE

3.1 FORMULATION

The linearized transonic theory reviewed in the previous section can be used to obtain the tunnel blockage interference over a model in a perforated tunnel as shown in Fig. 1b. The boundary conditions at the tunnel walls are assumed to be

or

$$\begin{aligned} \phi_x \pm T\phi_y &= 0 \text{ at } y = \pm h \\ u_x \pm T u_y &= 0 \text{ at } y = \pm h \end{aligned} \tag{12}$$

where T is the porosity parameter, an empirical constant for a given perforated wall. The boundary condition, Eq. (12), assumes that the mass flow is proportional to the pressure drop across the tunnel wall (Ref. 2). As with the free-air case, the boundary condition on the

airfoil is that the flow is tangent to the surface. Far upstream and downstream, the disturbance perturbation velocity vanishes. The linearized transonic equation of perturbation velocity is used for the field equation. Hence, the boundary value problem for the tunnel blockage interference can be described by Eqs. (4), (5), (6), and (12). The Fourier transform technique is applied in a manner similar to that of the free-air case. The solution of Eq. (4) in the transform plane is

$$\bar{u}(y,p) = C_1(p)\, e^{-\lambda y} + C_2(p)\, e^{\lambda y} \tag{13}$$

where the constants C_1 and C_2, determined by the transformed boundary conditions

and

$$-ip\bar{u} + T\bar{u}_y = 0 \qquad \text{at } y = h$$

$$\bar{u}_y = rf(p) \qquad \text{at } y \to 0$$

are of the form

$$C_1(p) = -\frac{rf(p)}{\lambda}\left[1 + \frac{(ip + T\lambda)\, e^{-\lambda h}}{(-ip + T\lambda)\, e^{\lambda h} - (ip + T\lambda)\, e^{-\lambda h}}\right] \tag{14}$$

$$C_2(p) = -\frac{rf(p)}{\lambda}\,\frac{(ip + T\lambda)\, e^{-\lambda h}}{(-ip + T\lambda)\, e^{\lambda h} - (ip + T\lambda)\, e^{-\lambda h}} \tag{15}$$

It is interesting to note that

$$C_1(p) = -rf(p)/\lambda$$

and

$$C_2(p) = 0$$

as

$$h \to \infty$$

so that Eq. (13) reduces to the free-air solution, Eq. (11), as expected. Substituting C_1 and C_2 into Eq. (13), the solution equation, one obtains

$$\bar{u} = \bar{u}_m - \frac{rf(p)}{\lambda}\,\frac{(ip + T\lambda)\, e^{-\lambda h}}{-ip\cosh\lambda h + T\lambda\sinh\lambda h}\cosh\lambda y$$

where $\bar{u}_m = -[rf(p)/\lambda]\, e^{-\lambda y}$, the solution for free-air flow in Eq. (11). Therefore, the interference velocity induced by the tunnel wall is

$$\bar{u}_i = \bar{u} - \bar{u}_m$$

$$= -\frac{rf(p)}{\lambda}\,\frac{(ip + T\lambda)\, e^{-\lambda h}}{-ip\cosh\lambda h + T\lambda\sinh\lambda h}\cosh\lambda y \tag{16}$$

In the physical plane, the interference velocity is obtained by the inverse formula,

$$u_i = \frac{\tau}{2\pi} i \int_{-\infty}^{\infty} \int_{-\infty}^{\infty} d\xi F_\xi \frac{p}{\lambda} \frac{(ip + T\lambda)\, e^{-\lambda h} \cosh \lambda y}{-ip \cosh \lambda h + T\lambda \sinh \lambda h} e^{-ip(x-\xi)}\, dp \qquad (17)$$

The interference velocity expression, Eq. (17), may be reduced to a real variable integration as follows:

$$\bar{u}_i = \frac{-\tau}{\pi} e^{\alpha x} \left[\int_0^{\infty} I_c(\omega, \alpha, T, h) \frac{e^{-\lambda h} \cosh \lambda y}{\lambda} M_c d\omega + \int_0^{\infty} I_s(\omega, \alpha, T, h) \frac{e^{-\lambda h} \cosh \lambda y}{\lambda} M_s d\omega \right] \qquad (18)$$

as shown in Appendix A, where $\lambda^2 = \beta^2(\omega^2 + \alpha^2)$ and $\alpha = k^2/2$. The expressions of I_C and I_S are listed in Appendix A. The qualities M_C and M_S are dependent on model geometry as

$$M_c = \int_{-\infty}^{\infty} F_\xi e^{-\alpha\xi} \cos \omega(x - \xi) d\xi$$

$$M_s = \int_{-\infty}^{\infty} F_\xi e^{-\alpha\xi} \sin \omega(x - \xi) d\xi \qquad (19)$$

For any given power series form of F_ξ, the model surface profile, the expressions for M_C and M_S may be integrated analytically and the interference velocity solution, Eq. (18), becomes a single integration which may be easily performed numerically.

3.2 DETERMINATION OF TRANSONIC ACCELERATION PARAMETER

In Eq. (18), one undetermined parameter, α, is directly related to the acceleration parameter as

$$\alpha = k^2/2 = \frac{(\alpha + 1)}{2} M_\infty^2 \tilde{\phi}_{xx}$$

In order to determine the value of the acceleration parameter, one assumes α to include two parts; thus,

$$\alpha = \alpha_1 + \alpha_2$$

where α_1 is induced by the model in free air and α_2 is induced by the presence of the tunnel wall.

The acceleration parameter α_1 is derived from the velocity solution in the free-air case (Ref. 12),

$$\alpha_1 = \frac{\pi}{2}\frac{\beta^5}{\tau(\gamma+1)M_\infty^2}\left[\tilde{\alpha}_1 K_1(\tilde{\alpha}_1)\sinh\tilde{\alpha}_1 - K_0(\tilde{\alpha}_1)(\cosh\tilde{\alpha}_1 - \sinh\tilde{\alpha}_1)\right] \tag{20}$$

where

$$\tilde{\alpha}_1 = \alpha_1/\beta^2$$

The acceleration parameter induced by the tunnel wall, α_2, is derived as follows by differentiating Eq. (18) with respect to x:

$$\alpha_2 = G(\alpha_1 + \alpha_2,\ x)$$

where

$$G(\alpha,x) = \alpha u_i(\alpha,T,x) - (2/\pi)^{1/2}\,\tau\, e^{\alpha x}\left[\int_0^\infty \frac{dM_c}{dx}\frac{e^{-\lambda h}}{\lambda} I_c\, d\omega + \int_0^\infty \frac{dM_s}{dx}\frac{e^{-\lambda h}}{\lambda} I_s\, d\omega\right] \tag{21}$$

Acceleration parameter α_1 is a constant averaged over the model, but parameter α_2 is a local acceleration dependent upon the chord location, x, along the model.

An iteration scheme is required to determine α_1 and α_2 from Eqs. (20) and (21). Once the acceleration parameter, α, is determined, the interference velocity can be calculated from Eq. (18).

4.0 INTERFERENCE PRESSURE ON A CIRCULAR-ARC AIRFOIL

A circular-arc airfoil was chosen as an example to calculate the interference pressure coefficient on a model in a perforated tunnel. The profile of a circular-arc airfoil is expressed as

$$\begin{aligned} F(\xi) &= 2\tau(\xi - \xi^2) \qquad 0 \le \xi \le 1 \\ &= 0 \qquad \text{elsewhere} \end{aligned} \tag{22}$$

where τ is the airfoil thickness ratio and the chord is a unit length. The quantities M_C and M_S of Eq. (19) may be determined from

$$M_c = \int_0^1 2\tau(1-2\xi)\, e^{-\alpha\xi}\cos\omega(x-\xi)\,d\xi \tag{23}$$

$$M_s = \int_0^1 2\pi(1 - 2\xi)\, e^{-\alpha\xi} \sin \omega(x - \xi) d\xi \tag{24}$$

The integrations of Eqs. (23) and (24) can be performed analytically, and the results are listed in Appendix B. The acceleration parameter, α, is calculated from Eqs. (20) and (21) with the expressions $\partial M_C/\partial_X$ and $\partial M_S/\partial_X$ easily obtained from M_C and M_S.

The pressure coefficient in the small perturbation theory is related to the axial perturbation velocity by $C_p = -2u$ where $u = u_i + u_m$; u_i = interference velocity of Eq. (18), and u_m = model-induced velocity in free air. Hence, the interference pressure coefficient may be expressed as

$$C_{p_i} = -2u_i \tag{25}$$

and may be related to the tunnel measured and free-air pressure coefficients by

$$C_{p_m} = C_{p_T} - C_{p_i} \tag{26}$$

where

C_{p_m} = model pressure coefficient in free air

and

C_{p_T} = measured pressure coefficient in the wind tunnel.

4.1 INTERFERENCE PRESSURE COEFFICIENT

The interference pressure coefficient for a circular-arc airfoil with 6-percent thickness ratio is shown in Fig. 2 for various tunnel porosity parameters, Q. The parameter Q is related to the porosity parameter, T, by $Q = (1 + \beta T)^{-1}$. For a closed tunnel, the value of Q is equal to zero, and for an open-jet tunnel, Q is equal to one. It may be seen from Fig. 2 that the sign of the interference pressure coefficients for closed and open-jet tunnels is opposite, as expected. It is also observed from Fig. 2 that as Mach number decreases, variation of interference pressure coefficient becomes rather uniform from the leading to the trailing edge of the airfoil, and the overall level of interference for a given value of tunnel porosity decreases.

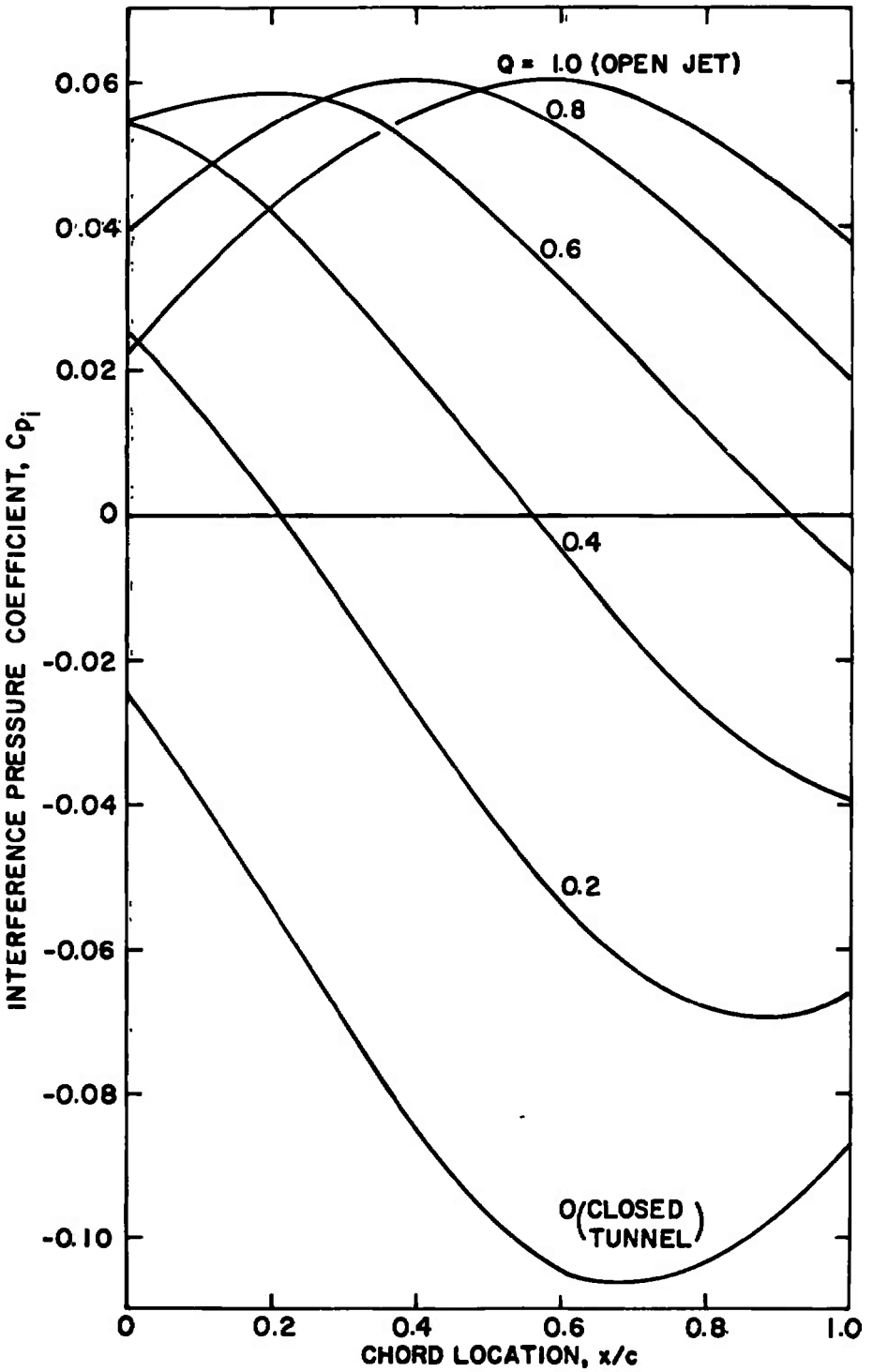

a. $M_\infty = 0.975$

Figure 2. Interference pressure coefficients on a 6-percent circular-arc airfoil at h/c = 3.0.

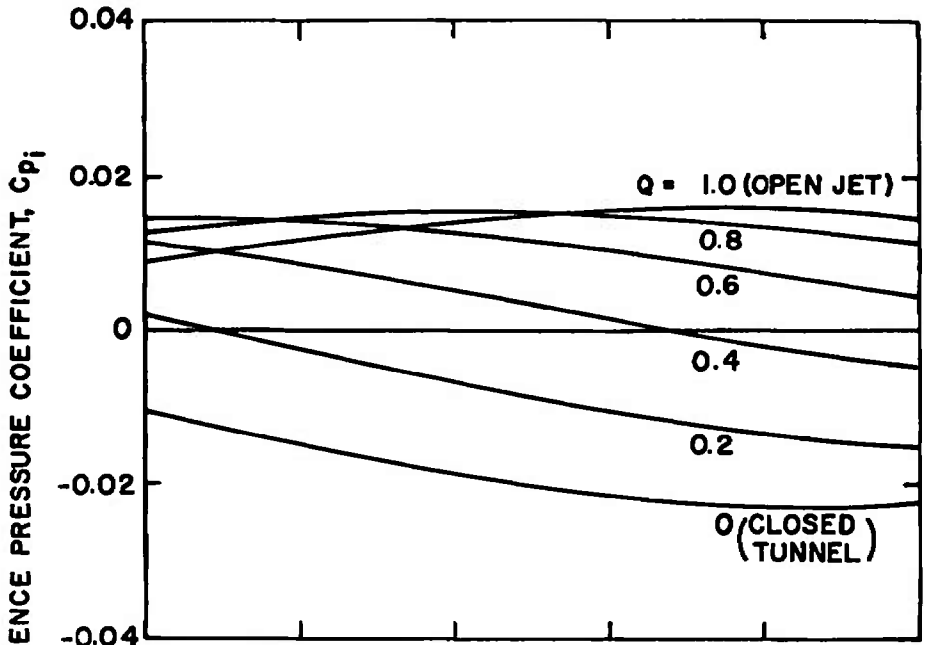

b. $M_\infty = 0.950$.

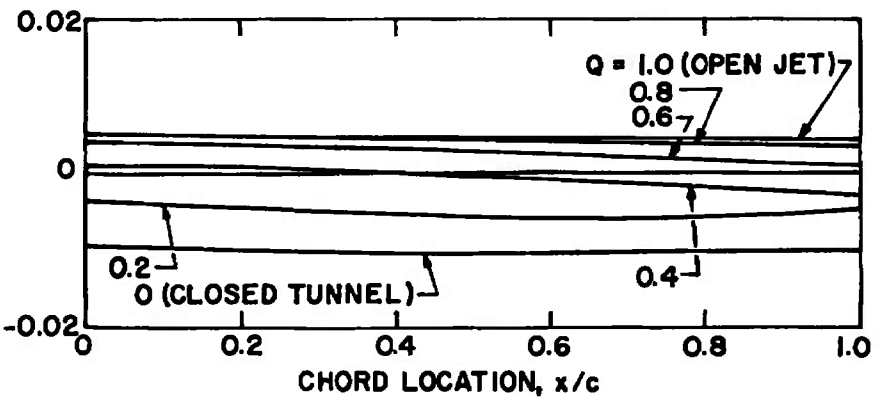

c. $M_\infty = 0.875$

Figure 2. Concluded.

The effect of tunnel height-to-chord ratio on the interference pressure coefficient is shown in Fig. 3. The interference pressure decreases as the parameter h/c increases. This trend is expected as the reduction of cross-section area blockage decreases the blockage interference.

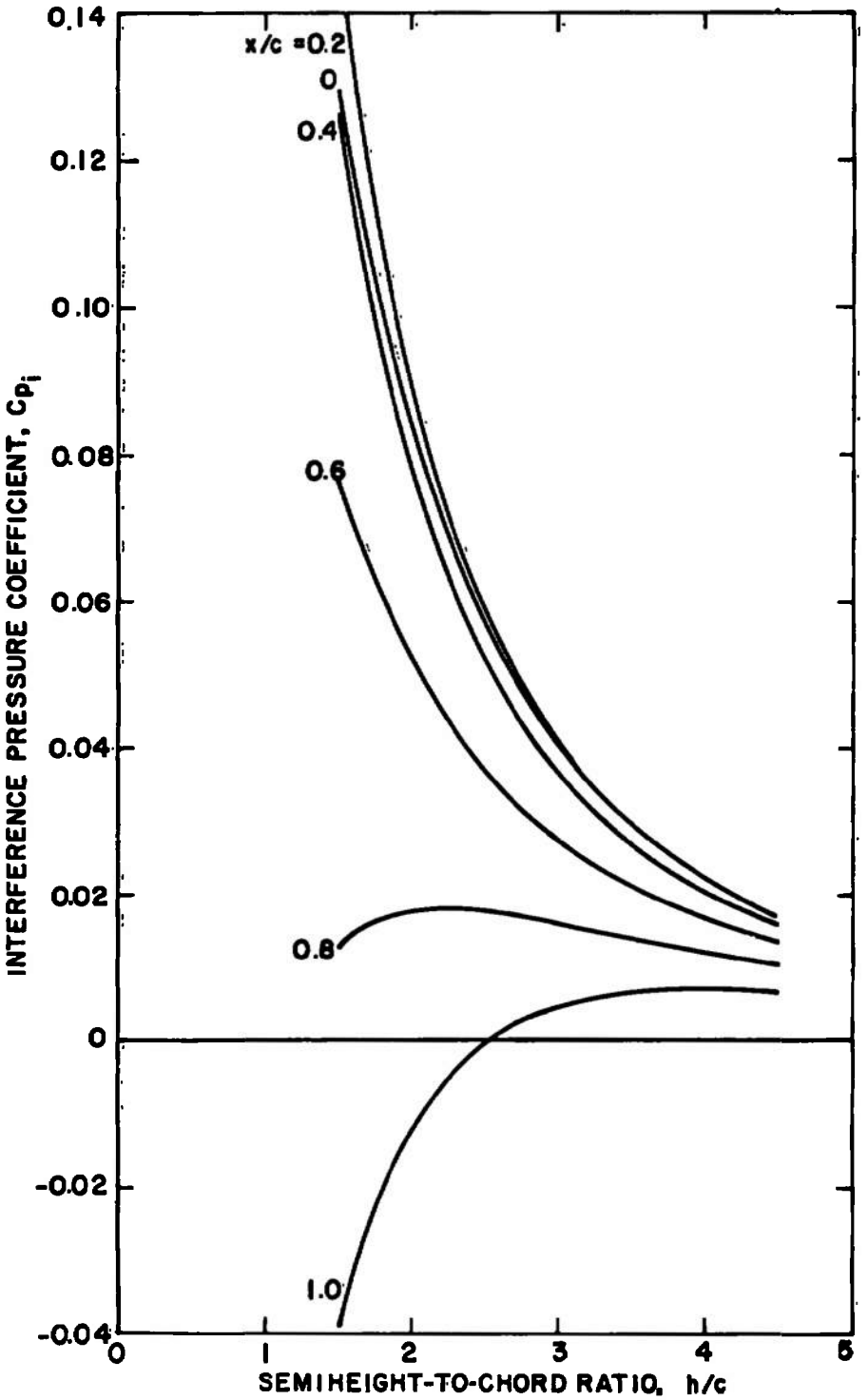

a. $M_\infty = 0.975$

Figure 3. Tunnel height to chord ratio effect on the interference pressure coefficient of a 6-percent circular-arc airfoil at Q = 0.6.

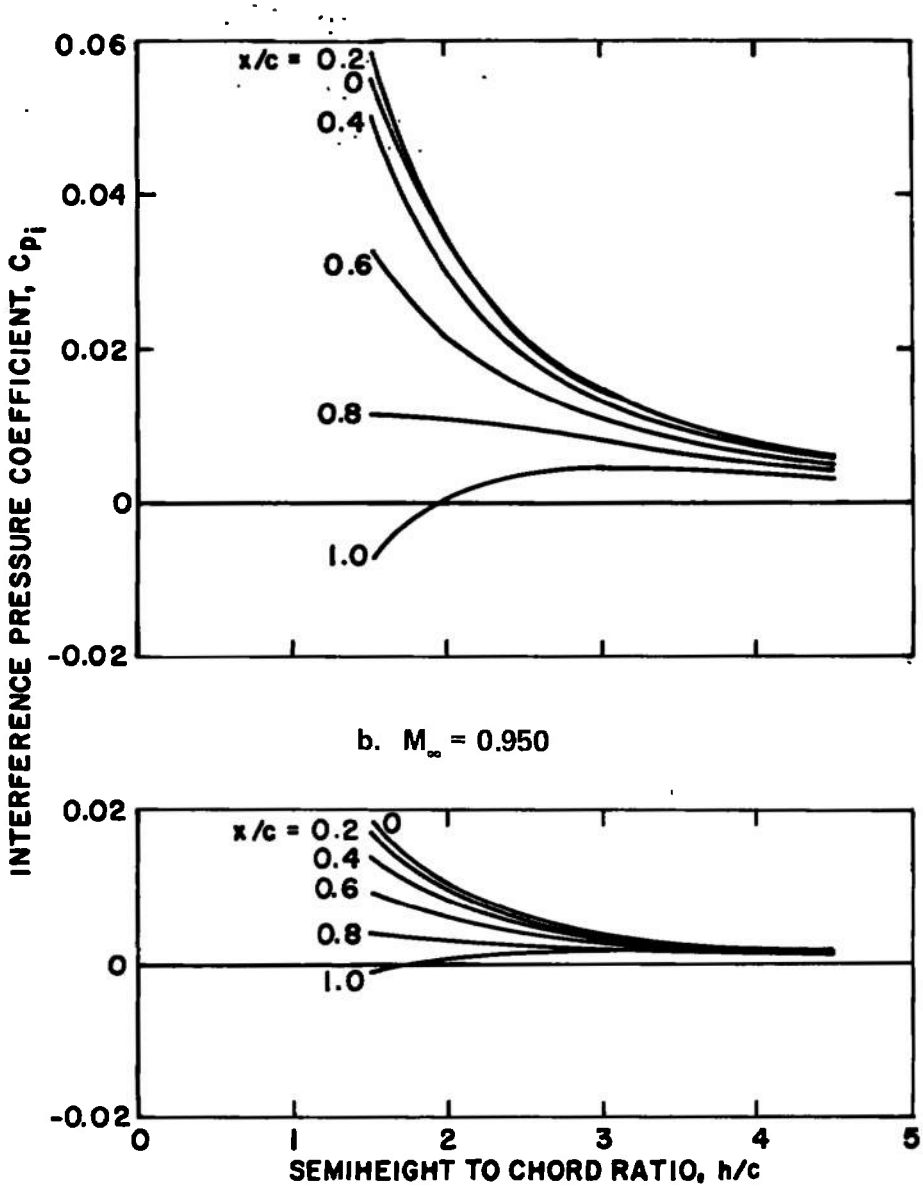

b. $M_\infty = 0.950$

c. $M_\infty = 0.875$

Figure 3. Concluded.

In order to evaluate the overall interference on the lift force of an airfoil, the average value of interference pressure coefficient over the airfoil chord is now introduced.

$$\widetilde{C}_{p_i} = \frac{1}{c}\int_o^c C_{p_i}\,dx \tag{27}$$

The value of $\tilde{C}_{p_i}$ plotted versus the porosity parameter, Q, is shown in Fig. 4 for various Mach numbers. The minimum value of $\tilde{C}_{p_i}$ occurs in the neighborhood of Q = 0.4 for several Mach numbers. It should be noted that the minimum value of $\tilde{C}_{p_i}$ implies only that the correction of the overall lift force is small.

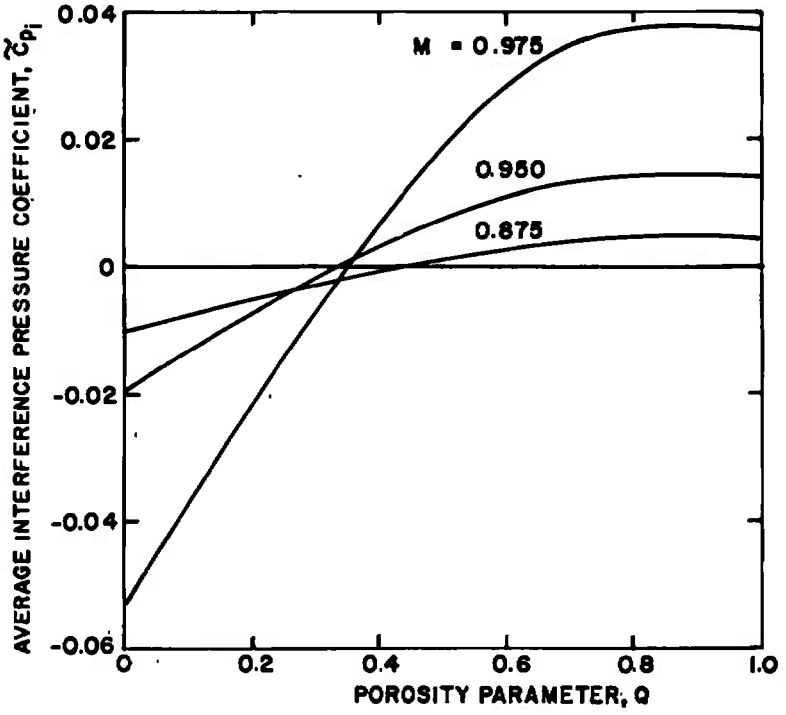

Figure 4. Porosity effect on the average interference pressure coefficient, $\tilde{C}_{p_i}$, of a 6-percent circular-arc airfoil at h/c = 3.0.

4.2 VALIDITY RANGE OF MACH NUMBER FOR SUBSONIC INTERFERENCE THEORY

The Mach number effect on the interference pressure coefficient is shown in Fig. 5 for several locations on the airfoil. The interference pressure coefficient, $\tilde{C}_{p_i}$, increases as Mach number increases. The results of subsonic wind tunnel theory are also shown in the same figure for the purpose of comparison with transonic theory.

The subsonic interference pressure is symmetrical about midchord for a closed tunnel and indicates in Fig. 5a that the interference pressures coincide at x/c = 0 and 1.0. The transonic interference theory

has no such symmetrical property. However, as Mach number decreases below 0.9, the interference pressure coefficients at the leading and trailing edges begin to merge. This indicates that the subsonic theory is valid at Mach numbers less than 0.9. It is also shown in Figs. 5b and c that the interference pressure coefficients of the subsonic theory deviate from the transonic theory at Mach numbers above 0.9. The results of subsonic theory overestimate the interference pressure above this Mach number, and the interference approaches infinity as the flow reaches sonic speed. Therefore, subsonic theory may be applicable for the blockage interference of a circular-arc airfoil up to Mach number 0.9. At Mach numbers greater than 0.9, the transonic wall interference theory should be used.

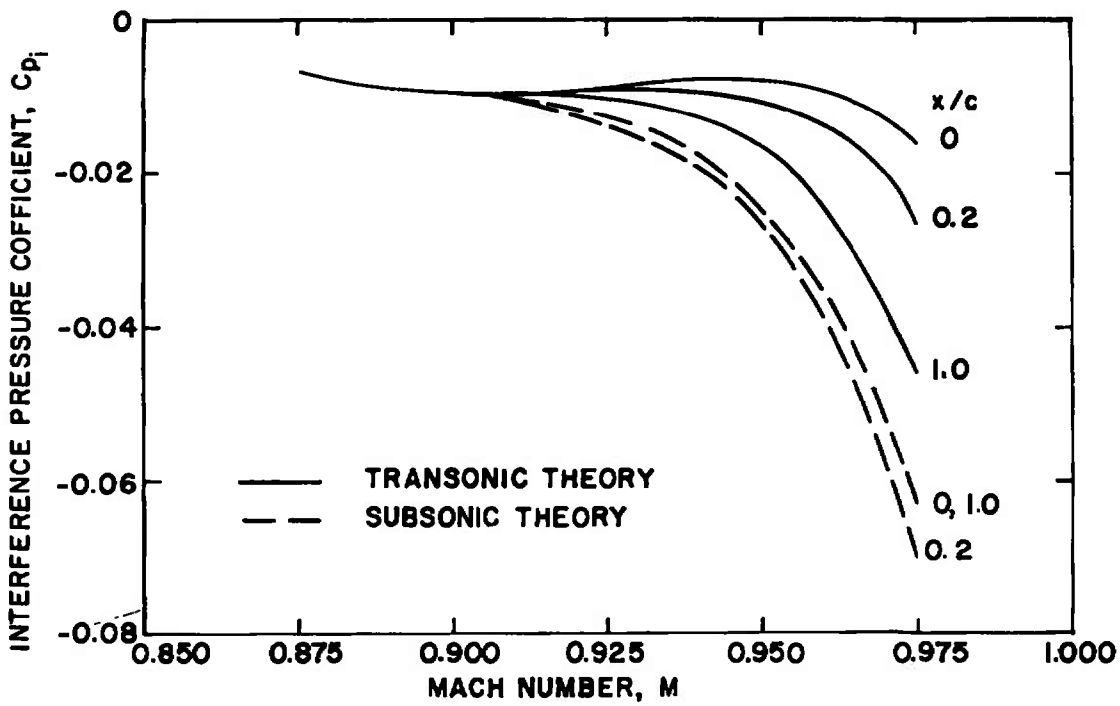

a. Q = 0 (closed tunnel), h/c = 3.5

Figure 5. Comparison of transonic and subsonic theories on interference pressure coefficient at various Mach numbers.

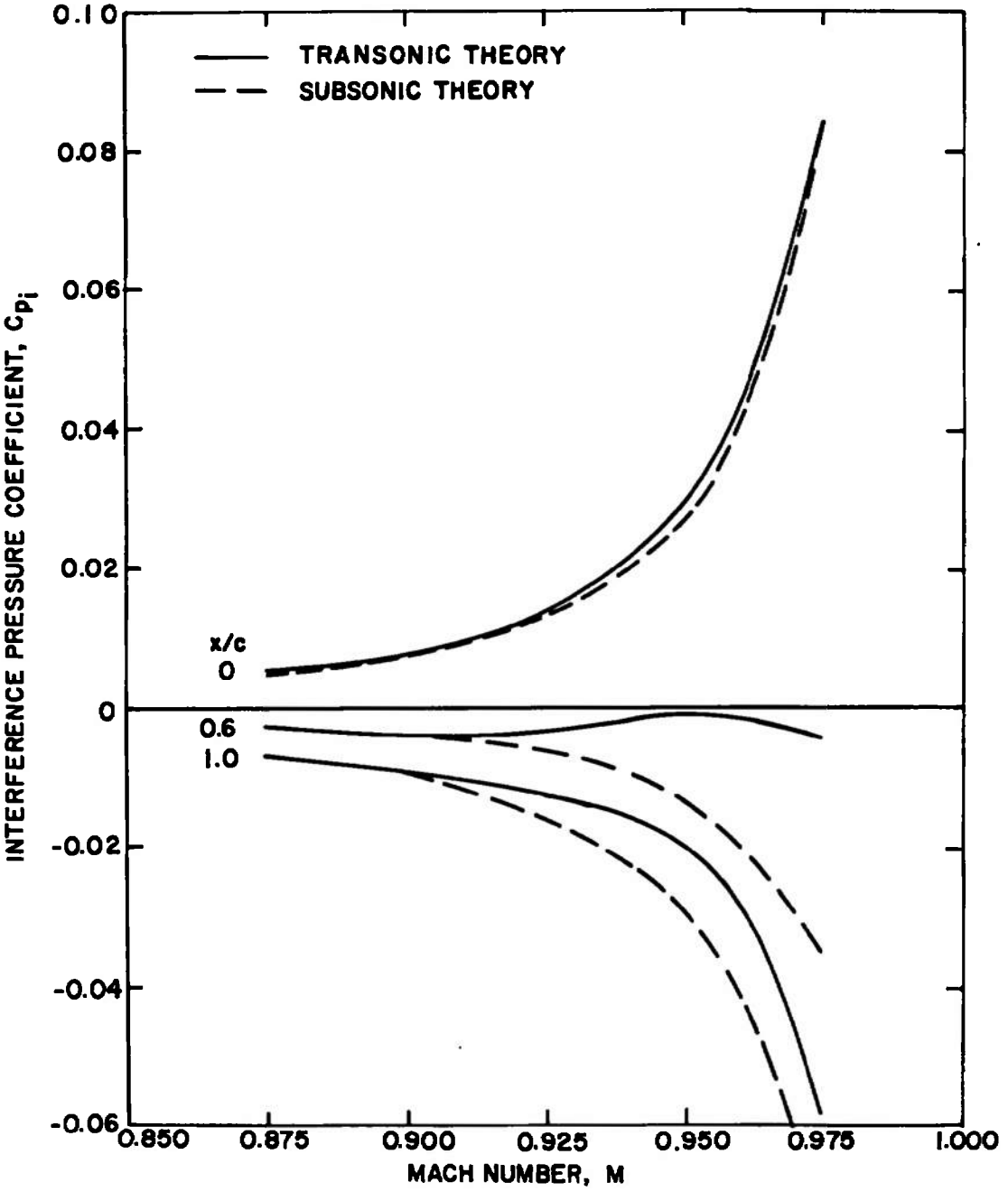

b. Q = 0.6, h/c = 1.5

Figure 5. Continued.

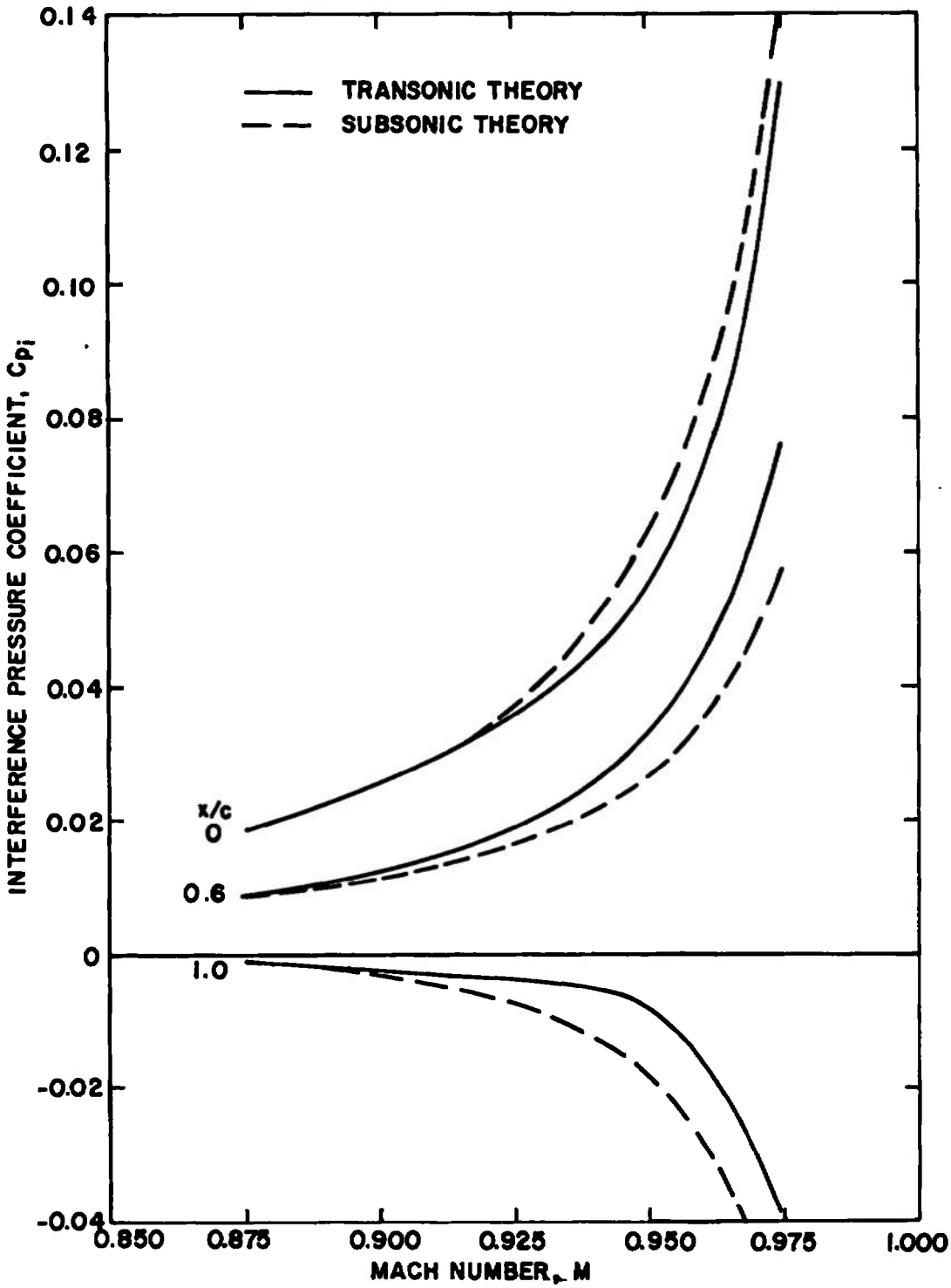

c. Ω = 0.5, h/c = 2.0

Figure 5. Concluded.

4.3 APPLICATION

The result of the interference pressure coefficient calculation may be used to correct wind tunnel data through Eq. (26). A set of data obtained by Collins (Ref. 13) in a closed tunnel with h/c = 3.4 at M_∞ = 0.915 is shown in Fig. 6a along with the free-air solution computed by Murman's numerical method (Ref. 8). It can be seen that the corrections improve the agreement between the data and the theoretical curve.

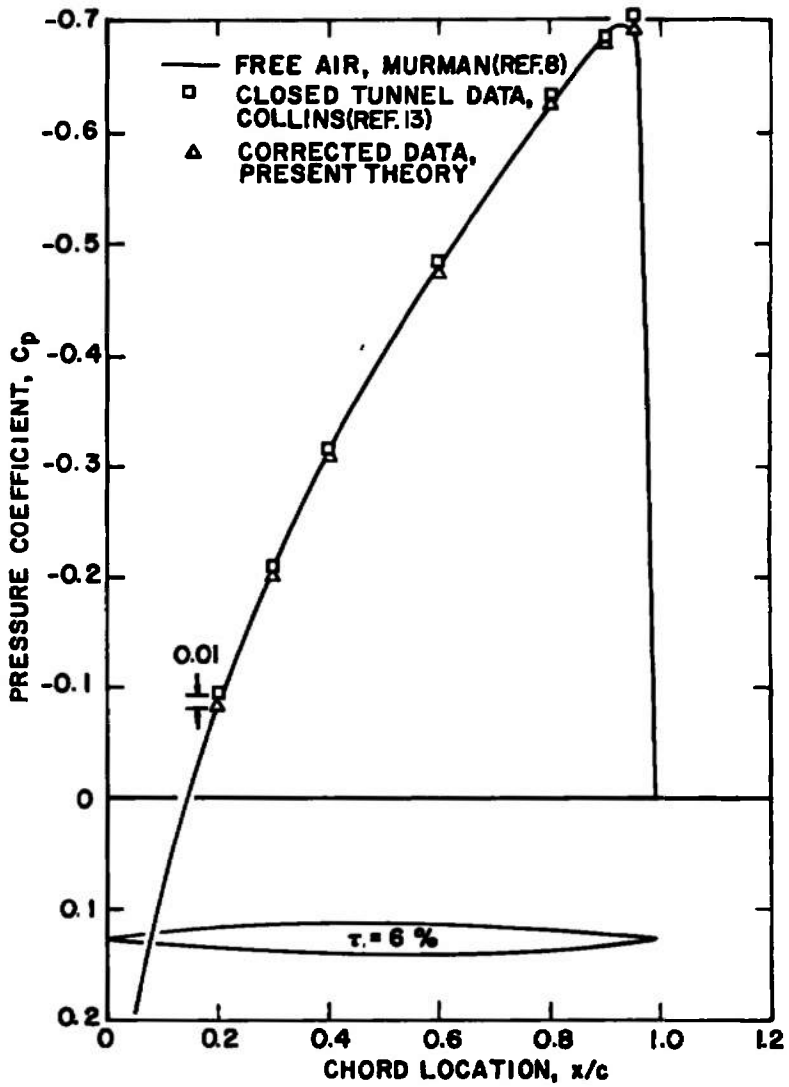

a. M = 0.915

Figure 6. Application of interference pressure coefficient to closed tunnel configuration on a 6-percent circular-arc airfoil at h/c = 3.4.

Further, it is shown in Fig. 6b that the present theory also accounts for the difference between free-air and closed tunnel theoretical solutions. It is noted, however, that the pressure near the trailing edge of the airfoil has a large gradient which indicates the appearance of a shock wave. The present correction theory is not applicable to the portion of the flow downstream of the shock wave location, since the linearized transonic theory does not permit a shock wave jump. However, the correction seems very good upstream of the shock wave.

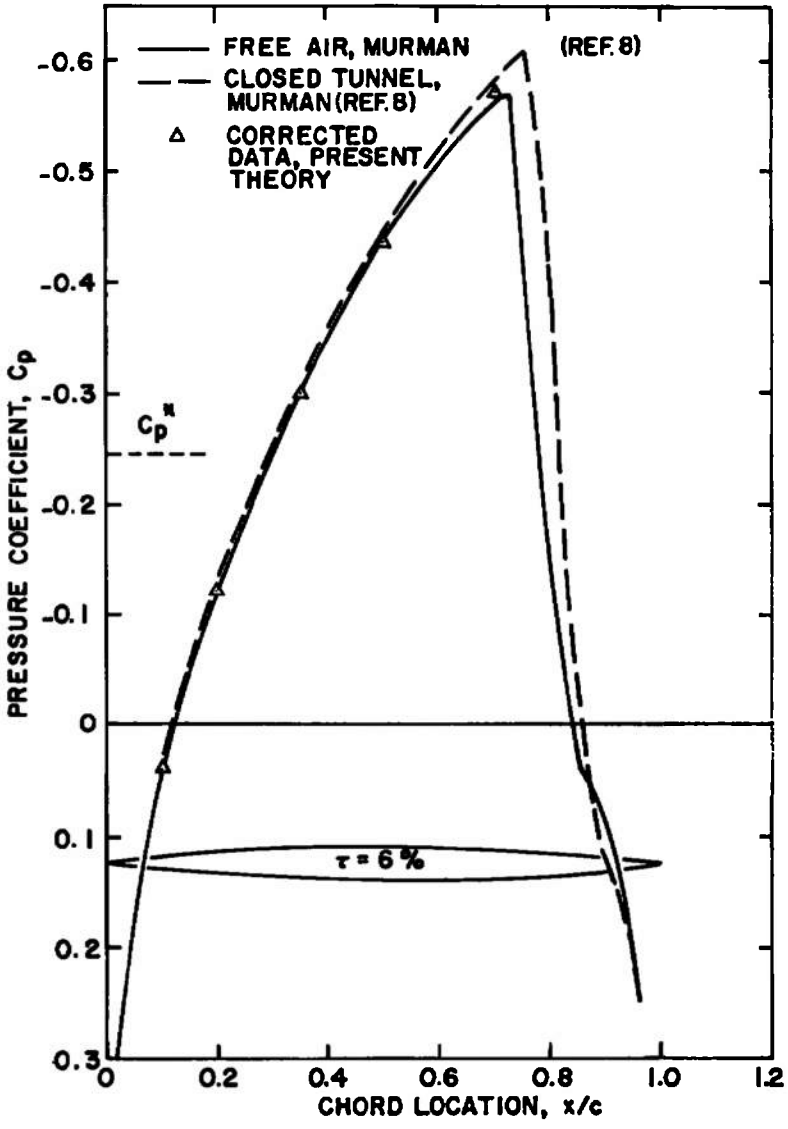

b. M = 0.875

Figure 6. Concluded.

5.0 CONCLUDING REMARKS

The transonic blockage interference was calculated in a perforated wall wind tunnel by the application of linearized transonic theory of Oswatitsch and Maeder.

The effects of the tunnel porosity parameter and tunnel height to airfoil chord ratio presented herein may provide some guideline in the selection of a tunnel wall configuration and model size. The determination of the applicable Mach number range for use of subsonic interference theory for a circular-arc airfoil has shown that subsonic interference theory can give good results beyond the critical Mach number of the airfoil. The application of transonic blockage interference corrections to two cases demonstrates that the present theory is very satisfactory. Future work is planned to extend the theory to consider bodies of revolution and also the lifting wing case.

REFERENCES

1. Garner, H. C. et al. "Subsonic Wind Tunnel Wall Corrections." AGARDograph 109, October 1966.

2. Pindzola, M. and Lo, C. F. "Boundary Interference at Subsonic Speeds in Wind Tunnels with Ventilated Walls." AEDC-TR-69-47 (AD687440), May 1969.

3. Lo, C. F. and Oliver, R. H. "Subsonic Lift Interference in a Wind Tunnel with Perforated Walls." Journal of Aircraft, Vol. 7, No. 3, May-June 1970, pp. 281-283.

4. Kraft, E. M. and Lo, C. F. "A General Solution for Lift Interference in Rectangular Ventilated Wind Tunnels." AIAA Journal, Vol. 11, No. 10, October 1973, pp. 1365-1366.

5. Berndt, S. B. "Theory of Wall Interference in Transonic Wind Tunnels." Symposium Transsonicum, Springer-Verlag, 1964, pp. 288-309.

6. Yoshihara, H. "Some Recent Developments in Planar Inviscid Transonic Airfoil Theory." AGARDograph-AG-156, February 1972.

7. Bailey, F. R. "Numerical Calculation of Transonic Flow about Slender Bodies of Revolution." NASA-TND-6582, December 1971.

8. Murman, E. M. "Computation of Wall Effects in Ventilated Transonic Wind Tunnels." AIAA Paper 72-1007, presented at the AIAA 7th Aerodynamics Testing Conference, Palo Alto, Calif., September 1972.

9. Chevalier, J. P. "Calculation of Wall Corrections for Transonic Wind Tunnels." A. A. A. F., 9th Applied Aerodynamics Colloquim, November 1972 (FTD-HC-23-351-73).

10. Goodman, T. R. "Wall Interference on Airfoils in Transonic Tunnels at Mach One." Oceanics, Inc., Report No. 73-95, May 1973.

11. Oswatitsch, K. "Flow Around Body of Revolution at Mach Number One." Brooklyn Polytechnic Institute Conference on High Speed Aeronautics, 1955.

12. Maeder, P. F. and Wood, A. D. "Linearized Transonic Flows Past Isolated Non-Lifting Airfoils." Brown University, TR-WT-24, June 1957.

13. Collins, D. J. and Krupp, J. A. "Experimental and Theoretical Investigations in Two-Dimensional Transonic Flow." AIAA Journal, Vol. 12, No. 6, June 1974, pp. 771-778.

APPENDIX A
EVALUATION OF THE INTERFERENCE VELOCITY EXPRESSION

The interference velocity expression, Eq. (17), is of the form

$$u_i = i\frac{r}{2\pi}\int_{-\infty}^{\infty}\int_{-\infty}^{\infty} d\xi\, F_\xi(\xi)\,\frac{p}{\lambda}\,\frac{(ip + T\lambda)\, e^{-\lambda h}\cosh \lambda y}{-ip\cosh \lambda h + T\lambda \sinh \lambda h}\, e^{-ip(x-\xi)}dp \qquad (A\text{-}1)$$

where

$$\lambda^2 = \beta^2 p(p - ik^2) \qquad (A\text{-}2)$$

From the physical argument, the interference velocity u_i must be a real value function, and the imaginary part should vanish by symmetrical properties. This will be verified later in this appendix.

Two additional variables, ω and α, are introduced as follows:

$$\begin{aligned}\lambda^2 &= \beta^2(\omega^2 + a^2)\\ &= \beta^2(\omega + i\alpha)(\omega - i\alpha)\end{aligned} \qquad (A\text{-}3)$$

From Eqs. (A-2) and (A-3), the following two equations are obtained:

$$p = \omega \mp i\alpha$$

$$p - ik^2 = \omega - i\alpha$$

where k^2 is a constant defined in Eq. (3). The new variable α becomes a constant parameter as $\alpha = k^2/2$ and the variable $\omega = p - i\alpha$. After the variables p and λ are replaced by the new variables ω and α, the interference equation, u_i, Eq. (A-1), may be simplified as a real value function.

$$u_i = \frac{-r}{\pi} e^{\alpha x}\left[\int_0^{\infty} d\omega\, I_c(\omega,\alpha,T,h)\,\frac{e^{-\lambda h}\cosh \lambda y}{\lambda}\int_{-\infty}^{\infty} F_\xi(\xi)\, e^{-\alpha\xi}\cos \omega(x-\xi)d\xi\right.$$

$$\left. + \int_0^{\infty} d\omega I_s(\omega,\alpha,T,h)\,\frac{e^{-\lambda h}\cosh \lambda y}{\lambda}\int_{-\infty}^{\infty} F_\xi(\xi)\, e^{-\alpha\xi}\sin \omega(x-\xi)d\xi\right] \qquad (A\text{-}4)$$

where

$$I_c = \frac{(\omega^2 - \alpha^2 + \alpha T\lambda)H + (T\lambda - 2\alpha)\omega^2 G}{H^2 + \omega^2 G^2}$$

$$I_s = \frac{-(T\lambda - 2\alpha)H - (\omega^2 - \alpha^2 + \alpha T\lambda)G}{H^2 + \omega^2 G^2}\,\omega$$

$$H = \alpha\cosh \lambda h + T\lambda \sinh \lambda h$$

$$G = \cosh \lambda h$$

$$\lambda = \beta\sqrt{\omega^2 + \alpha^2}$$

APPENDIX B
INTEGRATION OF EXPRESSIONS M_c AND M_s

Expressions M_C and M_S of Eqs. (23) and (24) for a circular-arc airfoil are integrated as follows:

$$M_c = 2\left(M_{c_1} - 2M_{c_2}\right)$$

where

$$M_{c_1} = -\frac{e^{-a\xi}}{a^2+\omega^2}\left[a\cos\omega(x-\xi) + \omega\sin\omega(x-\xi)\right]\Bigg|_{\xi=0}^{\xi=1}$$

and

$$M_{c_2} = -\frac{e^{-a\xi}}{a^2+\omega^2}\left[\left(a\xi + \frac{a^2-\omega^2}{a+\omega^2}\right)\cos\omega(x-\xi) + \left(\omega\xi + \frac{2a\omega}{a^2+\omega^2}\right)\sin\omega(x-\xi)\right]\Bigg|_{\xi=0}^{\xi=1}$$

$$M_s = 2M_{s_1} - 4M_{s_2}$$

where

$$M_{s_1} = \frac{e^{-a\xi}}{a^2+\omega^2}\left[-a\sin\omega(x-\xi) + \omega\cos\omega(x-\xi)\right]\Bigg|_{\xi=0}^{\xi=1}$$

and

$$M_{s_2} = -\frac{e^{-a\xi}}{a^2+\omega^2}\left[\left(a\xi + \frac{a^2-\omega^2}{a^2-\omega^2}\right)\sin\omega(x-\xi) - \left(\omega\xi + \frac{2a\omega}{a^2-\omega^2}\right)\cos\omega(x-\xi)\right]\Bigg|_{\xi=0}^{\xi=1}$$

$$[\quad]\Big|_{\xi=0}^{\xi=1} = [\quad]_{\xi=1} - [\quad]_{\xi=0}$$

NOMENCLATURE

$C_1(p)$, $C_2(p)$	Functions of p in Eqs. (14) and (15)
C_p	Pressure coefficient
C_p^*	Critical pressure coefficient
C_{p_i}	Average interference pressure coefficient, Eq. (27)
F(x)	Airfoil profile function
f(p)	Fourier transform of F_{xx}, Eq. (5)
h	Semiheight of tunnel
I_c, I_s	Functions defined in Appendix A
k^2	Acceleration constant
M_c, M_s	Functions defined in Appendix B
M_∞	Free-stream Mach number
p	Fourier transform parameter
Q	Porosity parameter, $(1 + \beta T)^{-1}$
T	Geometric porosity parameter
U_∞	Free-stream velocity
u	Perturbation axial velocity
x, y	Cartesian coordinates, Fig. 1
α	Acceleration parameter, $k^2/2$
α_1	Acceleration parameter, induced by model
α_2	Acceleration parameter, induced by tunnel wall
β	Compressibility parameter, $(1 - M_\infty^2)^{1/2}$
γ	Specific heat ratio
λ	$\beta^2 p(p - ik^2)^{1/2}$, Eq. (9)
ξ	Dummy variable
ϕ	Perturbation velocity potential
τ	Airfoil thickness ratio
ω	Dummy variable

SUBSCRIPTS

i	Interference
m	Model
T	Tunnel measured data
x, y, ξ	First derivative with respect to x, y, and ξ, respectively
xx, yy	Second derivative with respect to x and y, respectively
∞	Free-stream condition